A Comparison of Two Fat Suppressed Magnetic Resonance Imaging Pulse Sequences to Standard T2-Weighted Images for Brain Parenchymal Contrast and the Identification of Lesions in Dogs with Inflammatory Intracranial Disease

Benjamin D. Young, Joseph M. Mankin, John F. Griffin, Geoffrey T. Fosgate, Jennifer L. Fowler, Jonathan M. Levine

Key words: brain, dog, imaging, MRI, fat suppression

Running Head: Fat and Fluid Suppression on Brain MR in Dogs

Funding sources: none

Previous presentations or abstracts: none

ABSTRACT

T2-weighted sequences are commonly relied upon in magnetic resonance (MR) imaging protocols for the detection of brain lesions in dogs. Previously the effect of fluid suppression via fluid attenuated inversion recovery (FLAIR) has been compared to T2-weighting with mixed results. Short *tau* inversion recovery (STIR) has been reported to increase the detection of some CNS lesion in people. The purpose of the current study was to evaluate the effect of fat suppression on brain parenchymal contrast resolution and lesion detection in dogs. We compared three sequences: T2-weighted images (T2w), STIR, and T2-weighted fluid attenuated inversion recovery with chemical fat suppression (T2-FLAIR-FS) in dogs with meningoencephalitis. Dogs with meningoencephalitis and dogs with idiopathic epilepsy were retrospectively identified and anonymized. Evaluators recorded the presence or absence of lesions within 12 predetermined brain regions on randomized sequences, viewing and scoring each sequence individually. Additionally signal to noise ratios, contrast to noise ratios, and relative contrast were measured in a reference population. STIR sequences had the highest relative contrast between grey and white matter. While descriptively more lesions were identified by evaluators on T2-FLAIR-FS images, there was no statistical difference in the relative sensitivity of lesion detection between the sequences. Nor was there a statistical difference in false lesion detection within our reference population. STIR may be favored for enhanced anatomic contrast depiction in brain imaging. No benefit of the inclusion of a fat suppressed T2-weighted FLAIR sequence was found.

INTRODUCTION

Though much clinical attention is given to optimizing signal to noise ratio (SNR), it has been stated that contrast to noise ratio (CNR) may be the most important aspect of magnetic resonance (MR) image quality.[1] It is the relative contrast within an image that allows observers to differentiate tissues and likely lesions within tissue.[2] Each MR pulse sequence provides a different CNR, which changes with magnetic field strength, and relative contrast, which may not.[2] Fat suppression eliminates high signal from fat causing an expanded grayscale, thereby altering the signal of non-suppressed tissues.[3-5] Fat suppressed T2- and proton density- (PD) weighted sequences have been associated with increased sensitivity for detecting certain CNS lesions in people.[6-9]

Magnetic resonance (MR) imaging of the brain is now standard at many referral veterinary institutions for the clinical evaluation of dogs and cats with intracranial disease. In order to identify brain lesions with MR, an evaluator must recognize either structural alterations of anatomy (e.g., a mass) or changes in the parenchymal signal intensity. Imaging protocols are developed that include pulse sequences to provide optimal spatial resolution and enhance tissue contrast resolution. Subject tissue contrast is based on differences in MR relaxation times and intrinsic local tissue environments. Magnetic resonance pulse sequence protocols for canine and feline brain imaging have been previously reported and invariably include T2-weighted (T2w) sequences (spin echo or turbo spin echo).[10-20] The long repetition and echo times used in T2w sequences produce high signal intensity in tissues with long T2 relaxation times such as CSF or edema. Lesions with increased fluid content are often most conspicuous

on T2w images, making T2-weighting one of the most relied upon sequences for lesion detection.[18] However the high signal from both CSF and fat on T2w images can make superficial or periventricular lesions difficult to distinguish, highlighting the need for more sensitive imaging sequences.

Fluid attenuated inversion recovery (FLAIR) is an imaging sequence which is initiated by a 180^{o} inversion pulse, allowing the selective nulling of signal from pure fluids such as cerebrospinal fluid (CSF) and cysts. With magnetic field strengths above 1T, FLAIR images can be weighted to enhance either T1 or T2 characteristics. The T2-weighted FLAIR (T2-FLAIR) sequence produces high signal intensity in edematous lesions, similar to T2w, though with very low signal intensity from CSF. The benefit of T2-FLAIR for brain lesion detection has been previously studied with mixed results. T2-FLAIR was compared with T2w in dogs and cats with suspected intracranial disease.[21] The authors reported very similar overall lesion detection and sequence agreement between T2w and T2-FLAIR, the benefit of T2-FLAIR mainly being the identification of periventricular or intraventricular lesions and confirming cystic fluid within lesions.[21] Simultaneous viewing of both sequences was necessary to confidently identify some periventricular lesions. The authors suggested that in the large majority of patients, the addition of T2-FLAIR sequences would not likely improve lesion detection. However a different study found T2-FLAIR to be the most sensitive sequence for detecting brain lesions and predicting abnormal CSF in dogs with multifocal inflammatory intracranial disease as compared to T2w and both pre- and postcontrast T1-weighting.[22] In some of this study's cases, T2-FLAIR was the only sequence in which any lesions were detected.

The suppression of signal from fat is another technique that has been investigated for enhanced CNS lesion detection in both veterinary and human patients. The MR signal from fat is most commonly suppressed by either short *tau* inversion recovery (STIR), by applying frequency-selective chemical fat saturation, or by opposed phase fat suppression.[23, 24] To date the primary benefit of fat suppression techniques reported for veterinary CNS imaging has been for distinguishing lesions obscured by epidural, retrobulbar, paravertebral, or medullary bone fat in post-contrast enhanced T1-weighted sequences.[4, 5] However STIR has been reported to enhance detection of some brain and spinal cord parenchymal lesions in human patients.[6-9] At high (3T) MR field strengths, STIR is influenced by the additive effects of proton density, T1 relaxation, and T2 relaxation and has been reported to create both high brain-CSF contrast (like T2w) and high grey-white matter contrast (like proton density weighted images).[9] The routine use of STIR or fast STIR sequences in CNS imaging has been suggested by some in human diagnostic radiology because of its increased lesion detection over T2w.[9, 25-29]

The purpose of the current study was to evaluate fat suppressed T2-weighted or proton density-weighted sequences and the effect on brain parenchymal contrast resolution and lesion conspicuity in dogs. The authors of this paper are not aware of a previous comparison between STIR and either T2w or T2-FLAIR for brain lesion detection in dogs. In this retrospective and cross-sectional study, our hypotheses were that: (1) STIR and T2-FLAIR with chemical fat saturation (T2-FLAIR-FS) would provide higher tissue contrast resolution than T2w in dogs with idiopathic epilepsy, and (2) both STIR and T2-FLAIR-FS would identify more lesions than T2w in dogs with meningoencephalitis, suggesting a higher relative sensitivity.

MATERIALS AND METHODS

Medical records at the Texas A&M University Teaching Hospital were searched from October 2011 to March 2013 for dogs presenting with signs of intracranial neurological disease. To reduce the rate of lesion detection caused by the identification of defined masses, lesion scoring was limited to those with meningoencephalitis. For inclusion in the study, dogs were required to have antemortem brain MR at 3T and meet the criteria of one of two study populations: (1) dogs with idiopathic epilepsy (reference population), diagnosed by history of recurrent seizures (>2 events separated by at least 1 week in time), an age at seizure onset of 1-7 years, normal brain MRI and CSF analysis, and no remarkable changes on blood work (complete blood count, serum biochemistry, and ammonia);[20] or (2) dogs with meningoencephalitis (inflammatory disease population), diagnosed by inflammatory cerebrospinal fluid tap (>5 total nucleated cells/µL with total red blood cells/ µL <2500 or necropsy diagnosis) and no known neoplasia.[30, 31] These criteria were selected to emphasize the importance of tissue signal characteristics and sequence contrast resolution in lesion identification. The enrolled dogs in the inflammatory disease population were not required to have MR-detected lesions in the medical record.

The study was limited to the following pre-contrast turbo spin echo sequences: T2w, STIR, and T2-FLAIR-FS, each in the transverse plane. Studies were acquired on a 3.0T system (Magnetom Verio, Siemens Medical Solutions USA, Malvern, PA, USA). Sequence parameters were as follows: T2w (repetition time (TR) 4200-6300 ms, echo time (TE) 93-115 ms, slice thickness 2.5 mm, interslice gap 0.1-0.3 mm, matrix 256-320 x 139-272), STIR (TR 4000-5100 ms, TE 31-43

ms, inversion time (TI) 220 ms, slice thickness 2.5 mm, interslice gap 0.3 mm, matrix 256-320 x 205-241), T2-FLAIR-FS (TR 9000 ms, TE 92-95 ms, TI 2500 ms, slice thickness 2.5 mm, interslice gap 0.1-0.3 mm, matrix 256-320 x 139-197).

For an objective analysis of tissue contrast resolution, only the reference population (dogs with idiopathic epilepsy) was used in order to provide normal tissue margins and locations. Measurements were performed by one author (J.M.M.) on each animal at 4 sites of grey-white matter interface: the frontal lobes at the level of the caudate nuclei, the temporal lobes at the level of the interthalamic adhesion, the cingulate gyrus at the level of the corpus callosum, and the occipital lobe at the level of the tentorium cerebelli. At each site one T2w slice was selected, on which a region of interest (ROI) was manually placed in the grey matter and another in the white matter. The left hemisphere was selected for this analysis. Regions of interest were drawn to include as much of the grey or white matter at each location as possible without inclusion of other tissues. The mean voxel signal greyscale intensity of the ROI was recorded at each site for grey and then white matter. Commercial viewing software (Osirix version 5.5, OsiriX Imaging Software, OsiriX Foundation, Geneva, Switzerland) was used to replicate identical ROIs from the T2w slices to the corresponding STIR and T2-FLAIR-FS slices of the same patient (Figure 1). On each image where measurements were made, an ROI was placed in the adjacent air to measure noise. The mean signal intensity, standard deviation, signal to noise ratio (SNR), contrast to noise ratio (CNR), and relative contrast (RC) between grey and white matter was calculated for each location. Combining all ROIs, these variables were calculated for each sequence.

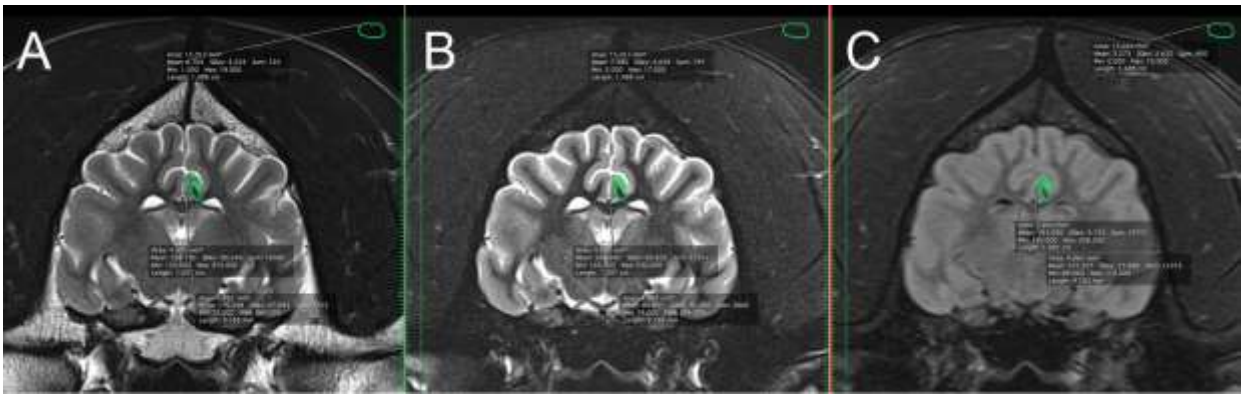

Figure 1. Transverse T2w (A), STIR (B), and T2-FLAIR-FS (C) MR images made at the level of the thalamus in a 3-year old mixed breed dog with idiopathic epilepsy. Regions of interest (ROI) have been manually placed in the grey and white matter of the left cingulate gyrus and in the adjacent air on the T2w images. The ROI's were then replicated in the corresponding locations of matched slices on the STIR and T2-FLIR-FS images.

The inflammatory disease and reference populations were combined to estimate the relative sensitivity for lesion detection. All sequences were anonymized and randomized by two investigators (J.L.F., B.D.Y.). All studies were evaluated in digital format by four investigators, two-board certified radiologists (B.D.Y., J.F.G) and two board certified neurologists (J.M.L., J.M.M.). Evaluators viewed only one sequence at a time. They were free to manipulate window width and level with full scrolling control, similar to clinical MR evaluation. Evaluators were able to determine the sequence type being viewed by virtue of the tissue signal characteristics, therefore no attempt was made to subjectively rate image quality. Sequences were reviewed individually in a blinded fashion. For the purpose of this study, 12 regions of the brain were considered: right and left portions of the telencephalon, diencephalon, mesencephalon, cerebellum, pons, and myelencephalon. The adjacent meninges were included in each brain

region. For every MR sequence, evaluators were asked to score each brain region: a score of 0 was given for no lesions detected; a score of 1 was given if any lesions were detected in the region, regardless of the number (Figure 2). This binary scoring for each region was chosen to account for the inherent difficulty of defining lesion boundaries and number. Thus, for each MR sequence, an evaluator could score a brain from 0-12 (i.e., a score of 12 would reflect one or more lesions in every brain region).

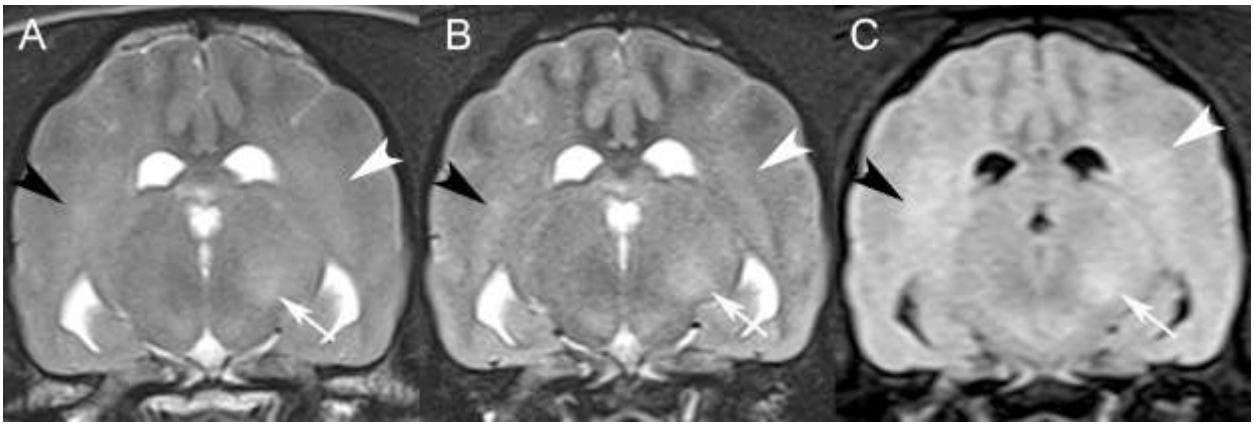

Figure 2. Transverse T2w (A), STIR (B), and T2-FLAIR-FS (C) MR images made at the level of the thalamus in a 4-year old West Highland White Terrier with granulomatous meningoencephalitis (GME). Evaluators could only review one anonymized and randomized MR sequence at a time. In each of these matched slices, hyperintense lesions are visible in the internal capsule of the right (black arrowheads) and left (white arrowheads) cerebral hemispheres and in the left thalamus (white arrows). There is also generalized loss of grey-white matter distinction in the temporal and pyriform lobes.

STATISTICAL ANALYSIS

All statistical analyses were selected and performed by one author (G.T.F.). The signal to noise ratio (SNR) was calculated as the signal intensity of the tissue divided by the standard deviation

of the signal intensity for the surrounding air.[2, 32] The contrast to noise ratio (CNR) was calculated as the (signal intensity of the gray matter minus the signal intensity of the white matter) divided by the standard deviation of the signal intensity for the surrounding air. The relative contrast (RC) was calculated as the (signal intensity of the gray matter minus the signal intensity of the white matter) divided by the signal intensity of the gray matter.[2] Signal intensity data were assessed for normality by calculating descriptive statistics, plotting histograms, and performing the Anderson-Darling test in commercially available software (MINITAB Statistical Software, Release 13.32, Minitab Inc, State College, Pennsylvania, USA). The effect of MR sequence on the signal intensity was estimated using linear mixed-models that included random effect terms for dog and image reviewer and fixed effects for brain location and MR sequence. The effect of MR sequence on the incorrect recognition of lesions in dogs with idiopathic epilepsy was estimated using mixed-effects logistic regression including random effects for dog and image reader and fixed effects for brain location and MR sequence. Similarly, the effect of MR sequence on the recognition of lesions in dogs diagnosed with intracranial inflammatory disease was estimated using mixed-effects logistic regression including random effects for dog and image reader and fixed effects for brain location and MR sequence. Multiple post-hoc pairwise comparisons were adjusted using the Bonferroni correction of P values. Statistical modelling was performed in commercially available software (IBM SPSS Statistics Version 21, International Business Machines Corp., Armonk, New York, USA) and results were interpreted at the 5% level of significance ($p \leq 0.05$). Kappa statistics were estimated independently for each MR sequence by entering standard formulas into a spreadsheet program as a measure of agreement among reviewers.[33]

RESULTS

A total of 46 dogs were included in the study. Sixteen dogs met the inclusion criteria of the reference population (diagnosed with idiopathic epilepsy). These included 2 male, 4 castrated male, 3 female, and 7 spayed female animals with a mean age of 3.5 years (range, 0.5-11 years). Breeds included mixed breed dogs (n=2) and one each of American Pit Bull Terrier, Australian Cattle Dog, Basset Hound, Belgian Malinois, Boxer, Cardigan Welsh Corgi, Catahoula Leopard Dog, Dalmatian, English Bulldog, Fox Terrier, French Bulldog, Maltese, Scottish Terrier, and Shih Tzu. Thirty dogs met the inclusion criteria for the inflammatory disease population. These included 2 male, 13 castrated male, 2 female, and 13 spayed female animals with a mean age of 4.6 years (range, 1-12 years). Breeds included American Pit Bull Terrier (1), Basset Hound (1), Border Collie (1), Boston Terrier (1), Cairn Terrier (1), Catahoula Leopard Dog, Chihuahua (3), Dachshund (2), English Setter, German Shepherd (2), Labrador Retriever (1), Maltese (3), Pekingese, Pomeranian Poodle (3), Rottweiler, Schnauzer, Shih Tzu (2), West Highland White Terrier (1), and Yorkshire Terrier (2). Specific neurological diagnoses were histologically or necropsy confirmed in some cases. Others were presumptive and based on clinical data including infectious disease titers, CSF, MRI features, and breed or other signalment features. Clinical diagnoses included granulomatous meningoencephalitis (GME, n=15), meningoencephalitis of unknown etiology (10), necrotizing meningoencephalitis (NME, 3), and aspergillosis (2).

In the 16 dogs with idiopathic epilepsy, the mean and SD for signal intensity, SNR, CNR, and relative contrast between grey and white matter are displayed for each location and each pulse

Table 1. Comparison of Contrast Between White and Grey Matter Among T2w, STIR, and T2W-FLAIR-FS Magnetic Resonance (MR) Sequences in 15 Dogs with Idiopathic Epilepsy.

Location	Tissue	Measure	MR sequence*			P-value†
			T2w	STIR	T2W-FLAIR-FS	
Cingulate	White	Values	193[a] (26)	110[b] (16)	213[a] (75)	<0.001
		SNR	61[a] (20)	35[b] (12)	68[a] (37)	<0.001
	Grey	Values	295[a] (47)	234[b] (31)	283[a,b] (90)	0.013
		SNR	94[a] (36)	74[b] (27)	90[a,b] (46)	0.032
	Contrast	CNR	34[a] (18)	39[a] (17)	22[b] (11)	<0.001
		RC (%)	34[a] (8)	52[b] (7)	25[c] (8)	<0.001
Frontal	White	Values	200[a] (25)	113[b] (14)	198[a] (69)	<0.001
		SNR	65[a] (18)	37[b] (11)	66[a] (37)	<0.001
	Grey	Values	264[a] (36)	205[b] (24)	252[a] (89)	0.004
		SNR	86[a] (25)	67[b] (19)	85[a,b] (50)	0.022
	Contrast	CNR	21[a] (9)	30[b] (9)	19[a] (13)	<0.001
		RC (%)	24[a] (5)	45[b] (4)	21[a] (4)	<0.001
Occipital	White	Values	212[a] (27)	131[b] (27)	251[c] (47)	<0.001
		SNR	64[a] (16)	40[b] (13)	78[c] (29)	<0.001
	Grey	Values	294[a] (54)	239[b] (50)	318[a] (68)	<0.001
		SNR	90[a] (26)	74[b] (26)	100[b] (41)	<0.001
	Contrast	CNR	25[a] (13)	34[b] (17)	21[a] (14)	<0.001
		RC (%)	27[a] (8)	45[b] (8)	21[c] (6)	<0.001
Temporal	White	Values	232[a] (39)	135[b] (21)	222[a] (52)	<0.001
		SNR	72[a] (22)	42[b] (13)	68[a] (20)	<0.001

	Grey	Values	301[a] (55)	221[b] (30)	270[a] (59)	<0.001
		SNR	93[a] (27)	68[b] (16)	83[a] (23)	<0.001
	Contrast	CNR	21[a] (8)	26[b] (7)	15[c] (6)	<0.001
		RC (%)	22[a] (6)	39[b] (8)	18[c] (5)	<0.001
Overall	White	Values	209[a] (33)	122[b] (22)	221[a] (63)	<0.001
		SNR	66[a] (19)	39[b] (12)	70[a] (31)	<0.001
	Grey	Values	289[a] (50)	225[b] (37)	281[a] (80)	<0.001
		SNR	91[a] (28)	71[b] (22)	89[a] (41)	<0.001
	Contrast	CNR	25[a] (14)	32[b] (14)	19[c] (12)	<0.001
		RC (%)	27[a] (8)	45[b] (8)	21[c] (6)	<0.001

*Data presented as mean (standard deviation).

†Based on mixed-effects linear regression. Means without suprascripts in common are significantly different after Bonferroni correction for multiple pairwise comparisons.

SNR = signal to noise ratio. CNR = contrast to noise ratio. RC = relative contrast.

sequence (Table 1). Overall, STIR images had the highest contrast to noise ratio (CNR) and relative contrast (RC), with T2w achieving the next highest, and T2-FLAIR-FS having the lowest CNR and CR. In each of the 4 areas where the grey and white matter were measured, STIR had the lowest signal to noise ratio (SNR) in both grey and white matter while T2w and T2-FLAIR-FS were not different.

In the 16 dogs with idiopathic epilepsy, the proportion of dogs with lesions incorrectly identified is displayed for each pulse sequence (Table 2). The incorrect recognition of lesions in dogs with idiopathic epilepsy was low, but highest in T2-FLAIR-FS (Table 2). However, no statistical differences in false lesion detection were recognized following correction for multiple

Table 2. Comparison of Magnetic Resonance (MR) Sequences for the Incorrect Recognition of Lesions in 16 Dogs with Idiopathic Epilepsy as Determined by Four Readers.

		T2w	STIR	T2W-FLAIR-FS	
Location	**Side**	**PI (95% CI)**	**PI (95% CI)**	**PI (95% CI)**	**P-value***
Cerebellum	Left	0 (0, 0.07)	0 (0, 0.07)	0.03 (0, 0.18)	0.814
	Right	0 (0, 0.07)	0 (0, 0.07)	0.03 (0, 0.18)	0.814
Diencephalon	Left	0 (0, 0.07)	0.03 (0.01, 0.12)	0.09 (0.02, 0.30)	0.372
	Right	0 (0, 0.07)	0.02 (0, 0.10)	0.09 (0.02, 0.30)	0.216
Mesencephalon	Left	0 (0, 0.07)	0.05 (0.01, 0.16)	0.11 (0.01, 0.43)	0.396
	Right	0 (0, 0.07)	0.03 (0.01, 0.12)	0.09 (0, 0.46)	0.337
Myelencephalon	Left	0.02 (0, 0.10)	0.05 (0.01, 0.16)	0.03 (0.01, 0.12)	0.861
	Right	0.02 (0, 0.10)	0.03 (0.01, 0.12)	0.05 (0.01, 0.16)	0.861
Pons	Left	0 (0, 0.07)	0.05 (0.01, 0.16)	0 (0, 0.07)	0.626
	Right	0 (0, 0.07)	0.03 (0.01, 0.12)	0 (0, 0.07)	0.814
Telencephalon	Left	0.03 (0.01, 0.12)	0.02 (0, 0.10)	0.16 (0.04, 0.39)	0.038
	Right	0.03 (0.01, 0.12)	0.03 (0.01, 0.12)	0.16 (0.04, 0.39)	0.053
All	Both	0.01 (0, 0.02)	0.03 (0.02, 0.04)	0.07 (0.04, 0.11)	<0.001

PI = proportion incorrect. CI = confidence interval.

*Based on mixed-effects logistic regression

Table 3. Comparison of Magnetic Resonance (MR) Sequences for the Recognition of Lesions (Relative Sensitivity) in 30 Dogs with Intracranial Inflammatory Disease as Determined by Four Readers.

		T2w	STIR	T2W-FLAIR-FS	
Location	**Side**	**PL (95% CI)**	**PL (95% CI)**	**PL (95% CI)**	**P-value***
Cerebellum	Left	0.23 (0.16, 0.32)	0.23 (0.16, 0.32)	0.35 (0.25, 0.46)	0.004
	Right	0.14 (0.09, 0.22)	0.13 (0.08, 0.21)	0.19 (0.13, 0.28)	0.137
Diencephalon	Left	0.30 (0.22, 0.39)	0.33 (0.23, 0.44)	0.35 (0.25, 0.46)	0.385
	Right	0.28 (0.20, 0.37)	0.30 (0.22, 0.39)	0.28 (0.21, 0.38)	0.787
Mesencephalon	Left	0.33 (0.23, 0.43)	0.35 (0.22, 0.51)	0.36 (0.21, 0.54)	0.639
	Right	0.28 (0.20, 0.37)	0.33 (0.23, 0.44)	0.33 (0.19, 0.51)	0.283
Myelencephalon	Left	0.30 (0.22, 0.39)	0.33 (0.24, 0.42)	0.34 (0.26, 0.44)	0.467
	Right	0.30 (0.22, 0.39)	0.32 (0.24, 0.41)	0.29 (0.21, 0.38)	0.739
Pons	Left	0.29 (0.21, 0.38)	0.32 (0.22, 0.43)	0.28 (0.18, 0.40)	0.446
	Right	0.25 (0.17, 0.35)	0.28 (0.19, 0.40)	0.24 (0.14, 0.38)	0.392
Telencephalon	Left	0.36 (0.27, 0.45)	0.36 (0.27, 0.45)	0.43 (0.34, 0.53)	0.047
	Right	0.32 (0.24, 0.41)	0.31 (0.23, 0.40)	0.41 (0.32, 0.50)	0.016
All	Both	0.28 (0.26, 0.30)	0.30 (0.27, 0.33)	0.32 (0.29, 0.36)	0.004

PL = proportion with identified lesions. CI = confidence interval

*Based on mixed-effects logistic regression

Table 4. Agreement Among 4 Readers for the Identification of Lesions in 16 Dogs with Idiopathic Epilepsy and 30 Dogs with intracranial inflammatory disease.

		T2w	STIR	T2W-FLAIR-FS
Location	**Side**	**kappa (95% CI)**	**kappa (95% CI)**	**kappa (95% CI)**
Cerebellum	Left	0.66 (0.55, 0.78)	0.64 (0.52, 0.75)	0.58 (0.46, 0.70)
	Right	0.81 (0.69, 0.92)	0.50 (0.38, 0.62)	0.58 (0.46, 0.70)
Diencephalon	Left	0.79 (0.68, 0.91)	0.68 (0.56, 0.79)	0.51 (0.39, 0.63)
	Right	0.74 (0.62, 0.86)	0.71 (0.60, 0.84)	0.45 (0.33, 0.56)
Mesencephalon	Left	0.73 (0.61, 0.85)	0.58 (0.46, 0.70)	0.47 (0.35, 0.59)
	Right	0.67 (0.55, 0.79)	0.59 (0.47, 0.71)	0.44 (0.32, 0.56)
Myelencephalon	Left	0.83 (0.71, 0.95)	0.71 (0.59, 0.83)	0.69 (0.56, 0.80)
	Right	0.83 (0.71, 0.95)	0.77 (0.65, 0.88)	0.69 (0.57, 0.81)
Pons	Left	0.78 (0.66, 0.90)	0.68 (0.56, 0.79)	0.72 (0.60, 0.84)
	Right	0.76 (0.64, 0.88)	0.68 (0.56, 0.80)	0.66 (0.54, 0.78)
Telencephalon	Left	0.76 (0.62, 0.85)	0.88 (0.76, 0.10)	0.48 (0.36, 0.60)
	Right	0.66 (0.54, 0.78)	0.75 (0.63, 0.87)	0.44 (0.33, 0.56)
Mean kappa	(SD)	0.75 (0.06)	0.68 (0.10)	0.56 (0.11)

CI = confidence interval. SD = standard deviation

pairwise comparisons. In the 30 dogs with inflammatory brain disease, the proportion of dogs with lesions identified is displayed for each pulse sequence (Table 3). There were no differences

in lesion detection between sequences in the inflammatory disease population following a correction for multiple pairwise comparisons. Data presented in Tables 2 and 3 are proportions and confidence intervals (CI) estimated from the pooled evaluations of all reviewers after adjustment for the repeated observations using mixed-effects statistical models. Agreement among observers was substantial for T2w and STIR and moderate for T2-FLAIR-FS (Table 4).

DISCUSSION

We hypothesized that STIR and T2-FLAIR-FS would have higher contrast resolution than T2w and would detect more lesions than T2w in dogs with meningoencephalitis. In our study, STIR had the highest CNR and relative contrast while T2-FLAIR-FS had the lowest. While descriptively more lesions were identified by evaluators on T2-FLAIR-FS images, there was no statistical difference in the relative sensitivity of lesion detection between the sequences. Nor was there a statistical difference in false lesion detection within our reference population. These findings are in agreement with one previous study that found no difference in lesion detection between T2w and T2-FLAIR.[21] In a different previous study, T2-FLAIR was more sensitive for identifying lesions in dogs with intracranial inflammatory disease, a finding our study did not replicate.[22] One difference between that study and the current study design was our addition of chemical fat saturation to the T2-FLAIR sequence. It is possible that this factor was responsible for the lack of significantly higher sensitivity of this sequence in the current study. A direct comparison of lesion detection of T2-FLAIR with and without fat saturation was not performed in this study and remains a possible topic for future investigation. The short echo times used in the STIR sequence created proton weighting, which the authors developed for use in routine diagnostic

cases due to its overall image contrast. In this study the evaluators favored the image quality of the STIR sequence and found the T2-FLAIR-FS least favorable. This likely reflects our finding of highest relative contrast in STIR and lowest in T2-FLAIR-FS. STIR is known for providing high anatomic detail of the brain in human patients, allowing enhanced surgical planning for superficial brain tumors.[9] It has been compared to the high resolution T2-reversed MRI, which offers superior anatomic detail.[9, 34, 35] Additionally the high contrast resolution of STIR has allowed improved diagnosis of parenchymal CNS lesions such as spinal cord multiple sclerosis plaques.[6, 8, 36, 37] The routine inclusion of STIR in brain MR protocols has been recommended for the evaluation of demyelinating diseases in children with epilepsy.[25] However in our study, the superior contrast resolution of STIR did not improve lesion detection in dogs with meningoencephalitis.

The three sequences evaluated differed in relative contrast and CNR, though these factors did not significantly impact the relative sensitivity of lesion detection. However evaluators had notably higher agreement in lesion detection when viewing each of the 2 sequences with higher relative contrast and CNR (STIR and T2w) compared to T2-FLAIR-FS. It is notable that while not statistically different, descriptively more false lesions were identified by evaluators on T2-FLAIR-FS. Combined with the results of the agreement analysis, it may be surmised that STIR enhances definition of anatomy while the T2-FLAIR-FS enhanced the variation in parenchymal signal intensity, sometimes to the detriment of accuracy.

One potential limitation of this study arises from our study design, which was selected to optimize the importance of tissue signal intensity over architectural change for brain lesion

detection. The purpose was to compare as closely as possible the diagnostic effect of pulse sequence relative contrast. It was presumed that masses, especially those with defined margins, represent the lesion type that is least dependent on subtle differences in signal intensity to detect. Only records from animals with meningoencephalitis were searched in creation of the group with expected lesions, because masses are found less commonly in inflammatory brain disease than in neoplastic or vascular brain diseases, and inflammatory brain lesions rarely have defined margins.[11, 38] However we did not exclude animals with mass effect, and therefore did not eliminate the influence of mass effect on lesion detection altogether. Also the relative sensitivity in detection of other disease categories was not evaluated. No histological confirmation of disease etiology was required in either the inflammatory disease population or the reference population of presumed idiopathic epileptic dogs. The designation of "false" lesions identified in our reference population depended on the correct diagnosis of structurally normal brains in this group. However these dogs met standard clinical criteria for the diagnosis of idiopathic epilepsy, and with access to the entire MR studies for cross reference, no lesions had been identified in these dogs previously. Another potential source of error was the binary scoring method for each brain region (i.e., score of either 0 for no lesions or 1 for any number of lesions). We were compelled to create a scoring system that reflected the fact that multifocal inflammatory lesions typically cannot be delineated, and that perilesional T2 hyperintensity (edema) limits one's ability on MR to distinguish true histologic brain lesion margins (i.e., 2 closely positioned lesions in one brain region might appear as either one lesion or 2, depending on the edema surrounding them).[39-41] Therefore our method

evaluated the number of brain regions affected with lesions and may have underestimated a difference in total number of brain lesions.

In conclusion, the addition of a STIR sequence to a standard MR brain imaging protocol may be favored for enhanced anatomic contrast depiction, but we identified no increase in relative sensitivity for detection of brain lesions. It may be of most benefit for enhancing identification of lesions obscured by extradural or medullary fat. No increase in lesion detection was identified by the application of chemical fat suppression to a T2-FLAIR sequence nor was it favored for image quality.

ACKNOWLEDGEMENTS

The authors would like to thank Wade Friedeck for MR sequence development, and Elizabeth Scanlin for data collection.

REFERENCES

1. McRobbie DW. *MRI from Picture to Proton*: Cambridge University Press, 2007.
2. Maubon AJ, Ferru JM, Berger V, Soulage MC, DeGraef M, Aubas P, et al. Effect of field strength on MR images: comparison of the same subject at 0.5, 1.0, and 1.5 T. Radiographics 1999; 19: 1057-1067.
3. Georgy BA, Hesselink JR, Middleton MS. Quantitative analysis of signal intensities and contrast after fat suppression in contrast-enhanced magnetic resonance imaging of the spine. Acad Radiol 1996; 3: 731-734.
4. D'Anjou MA, Carmel EN, Tidwell AS. Value of fat suppression in gadolinium-enhanced magnetic resonance neuroimaging. Vet Radiol Ultrasound 2011; 52: S85-90.
5. D'Anjou MA, Carmel EN, Blond L, Beauchamp G, Parent J. Effect of acquisition time and chemical fat suppression on meningeal enhancement on MR imaging in dogs. Vet Radiol Ultrasound 2012; 53: 11-20.

6. Rocca MA, Mastronardo G, Horsfield MA, Pereira C, Iannucci G, Colombo B, et al. Comparison of three MR sequences for the detection of cervical cord lesions in patients with multiple sclerosis. AJNR Am J Neuroradiol 1999; 20: 1710-1716.
7. Mascalchi M, Dal Pozzo G, Bartolozzi C. Effectiveness of the Short TI Inversion Recovery (STIR) sequence in MR imaging of intramedullary spinal lesions. Magn Reson Imaging 1993; 11: 17-25.
8. Dietemann JL, Thibaut-Menard A, Warter JM, Neugroschl C, Tranchant C, Gillis C, et al. MRI in multiple sclerosis of the spinal cord: evaluation of fast short-tan inversion-recovery and spin-echo sequences. Neuroradiology 2000; 42: 810-813.
9. Beppu T, Inoue T, Nishimoto H, Ogasawara K, Ogawa A, Sasaki M. Preoperative imaging of superficially located glioma resection using short inversion-time inversion recovery images in high-field magnetic resonance imaging. Clin Neurol Neurosurg 2007; 109: 327-334.
10. Cervera V, Mai W, Vite CH, Johnson V, Dayrell-Hart B, Seiler GS. Comparative magnetic resonance imaging findings between gliomas and presumed cerebrovascular accidents in dogs. Vet Radiol Ultrasound 2011; 52: 33-40.
11. Cherubini GB, Mantis P, Martinez TA, Lamb CR, Cappello R. Utility of magnetic resonance imaging for distinguishing neoplastic from non-neoplastic brain lesions in dogs and cats. Vet Radiol Ultrasound 2005; 46: 384-387.
12. Kraft SL, Gavin PR. Intracranial neoplasia. Clin Tech Small Anim Pract 1999; 14: 112-123.
13. Kraft SL, Gavin PR, DeHaan C, Moore M, Wendling LR, Leathers CW. Retrospective review of 50 canine intracranial tumors evaluated by magnetic resonance imaging. J Vet Intern Med 1997; 11: 218-225.
14. Lamb CR, Croson PJ, Cappello R, Cherubini GB. Magnetic resonance imaging findings in 25 dogs with inflammatory cerebrospinal fluid. Vet Radiol Ultrasound 2005; 46: 17-22.
15. McConnell JF, Garosi L, Platt SR. Magnetic resonance imaging findings of presumed cerebellar cerebrovascular accident in twelve dogs. Vet Radiol Ultrasound 2005; 46: 1-10.
16. Negrin A, Lamb CR, Cappello R, Cherubini GB. Results of magnetic resonance imaging in 14 cats with meningoencephalitis. J Feline Med Surg 2007; 9: 109-116.
17. Palus V, Volk HA, Lamb CR, Targett MP, Cherubini GB. MRI features of CNS lymphoma in dogs and cats. Vet Radiol Ultrasound 2012; 53: 44-49.
18. Robertson I. Optimal magnetic resonance imaging of the brain. Vet Radiol Ultrasound 2011; 52: S15-22.
19. Wisner ER, Dickinson PJ, Higgins RJ. Magnetic resonance imaging features of canine intracranial neoplasia. Vet Radiol Ultrasound 2011; 52: S52-61.
20. Wolff CA, Holmes SP, Young BD, Chen AV, Kent M, Platt SR, et al. Magnetic resonance imaging for the differentiation of neoplastic, inflammatory, and cerebrovascular brain disease in dogs. J Vet Intern Med 2012; 26: 589-597.
21. Benigni L, Lamb CR. Comparison of fluid-attenuated inversion recovery and T2-weighted magnetic resonance images in dogs and cats with suspected brain disease. Vet Radiol Ultrasound 2005; 46: 287-292.
22. Cherubini GB, Platt SR, Howson S, Baines E, Brodbelt DC, Dennis R. Comparison of magnetic resonance imaging sequences in dogs with multi-focal intracranial disease. J Small Anim Pract 2008; 49: 634-640.
23. Delfaut EM, Beltran J, Johnson G, Rousseau J, Marchandise X, Cotten A. Fat suppression in MR imaging: techniques and pitfalls. Radiographics 1999; 19: 373-382.
24. Tien RD. Fat-suppression MR imaging in neuroradiology: techniques and clinical application. AJR Am J Roentgenol 1992; 158: 369-379.
25. Gupta V, Bronen RA. Epilepsy. In: Atlas SW (ed): *Magnetic resonance imaging of the brain and spine*: Lippincott, Williams and Wilkins, 2009;307-342.

26. Inoue T, Ogasawara K, Beppu T, Ogawa A. Three-dimensional anisotropy contrast imaging of gliomatosis cerebri: two case reports. Surg Neurol 2004; 62: 151-154; discussion 154-155.
27. Oikawa H, Sasaki M, Tamakawa Y, Ehara S, Tohyama K. The substantia nigra in Parkinson disease: proton density-weighted spin-echo and fast short inversion time inversion-recovery MR findings. AJNR Am J Neuroradiol 2002; 23: 1747-1756.
28. Sasaki M, Inoue T, Tohyama K, Oikawa H, Ehara S, Ogawa A. High-field MRI of the central nervous system: current approaches to clinical and microscopic imaging. Magn Reson Med Sci 2003; 2: 133-139.
29. Sawaishi Y, Sasaki M, Yano T, Hirayama A, Akabane J, Takada G. A hippocampal lesion detected by high-field 3 tesla magnetic resonance imaging in a patient with temporal lobe epilepsy. Tohoku J Exp Med 2005; 205: 287-291.
30. Nghiem PP, Schatzberg SJ. Conventional and molecular diagnostic testing for the acute neurologic patient. J Vet Emerg Crit Care (San Antonio) 2010; 20: 46-61.
31. Talarico LR, Schatzberg SJ. Idiopathic granulomatous and necrotising inflammatory disorders of the canine central nervous system: a review and future perspectives. J Small Anim Pract 2010; 51: 138-149.
32. Kang BT, Ko KJ, Jang DP, Han JY, Lim CY, Park C, et al. Magnetic resonance imaging of the canine brain at 7 T. Vet Radiol Ultrasound 2009; 50: 615-621.
33. Fleiss JL, Levin B, Paik MC. *Statistical Methods for Rates and Proportions*: Wiley and Sons, 2013.
34. Fujii Y, Nakayama N, Nakada T. High-resolution T2-reversed magnetic resonance imaging on a high magnetic field system. Technical note. J Neurosurg 1998; 89: 492-495.
35. Nakada T, Kwee IL, Fujii Y, Knight RT. High-field, T2 reversed MRI of the hippocampus in transient global amnesia. Neurology 2005; 64: 1170-1174.
36. Bot JC, Barkhof F, Lycklama a Nijeholt GJ, Bergers E, Polman CH, Ader HJ, et al. Comparison of a conventional cardiac-triggered dual spin-echo and a fast STIR sequence in detection of spinal cord lesions in multiple sclerosis. Eur Radiol 2000; 10: 753-758.
37. Campi A, Pontesilli S, Gerevini S, Scotti G. Comparison of MRI pulse sequences for investigation of lesions of the cervical spinal cord. Neuroradiology 2000; 42: 669-675.
38. Young BD, Fosgate GT, Holmes SP, Wolff CA, Chen-Allen AV, Kent M, et al. Evaluation of Standard Magnetic Resonance Characteristics Used to Differentiate Neoplastic, Inflammatory, and Vascular Brain Lesions in Dogs. Vet Radiol Ultrasound 2014.
39. Earnest Ft, Kelly PJ, Scheithauer BW, Kall BA, Cascino TL, Ehman RL, et al. Cerebral astrocytomas: histopathologic correlation of MR and CT contrast enhancement with stereotactic biopsy. Radiology 1988; 166: 823-827.
40. Jayaraman MV, Boxerman JL. Adult Brain Tumors. In: Atlas SW (ed): *Magnetic Resonance Imaging of the Brain and Spine*: Lippincott, Williams and Wilkins, 2009;4445-4590.
41. Kelly PJ, Daumas-Duport C, Kispert DB, Kall BA, Scheithauer BW, Illig JJ. Imaging-based stereotaxic serial biopsies in untreated intracranial glial neoplasms. J Neurosurg 1987; 66: 865-874.